

Chapter 17

Nanocomposites Potential for Aero Applications

Naveen K. Mahenderkar, T. Ram Prabhu and Anil Kumar

Abstract This chapter briefly summarizes the types of nanocomposites, their fabrication and properties. Emphasis is placed on the strengthening mechanisms for metal, polymer and ceramic matrix nanocomposites. A brief introduction to the types of reinforcement and matrix materials is given, and finally the current developments and future trends of nanocomposites are discussed.

Keywords Nanocomposites · Metal matrix · Polymer matrix · Ceramic matrix · Processing · Applications

17.1 Introduction

Nanocomposites are materials similar to conventional composites with a matrix phase and a reinforcement phase, although unlike conventional composites the dimensions of reinforcement materials are typically on the order of 100 nm or less. The reinforcement are usually 1-D, 2-D or 3-D nanomaterials.

Nanocomposites are a fast growing area of research and application owing to their unique properties that are usually not seen in conventional composite materials. The properties of nanocomposites depend on both the matrix and reinforcement phases and are also influenced by the morphology and interfacial characteristics. Research so far showed that virtually all types of nanocomposites

N.K. Mahenderkar (✉)

Department of Materials Science and Engineering, Missouri University of Science and Technology, Rolla, MO, USA
e-mail: nm53f@mst.edu

T. Ram Prabhu (✉)

RCMA (F&F-FOL), CEMILAC, Hyderabad, India
e-mail: ramprabhu.t@gmail.com

A. Kumar

ASL, DRDO, Hyderabad, India
e-mail: anil_drld43@hotmail.com

show improved properties compared to their conventional counterparts. Therefore nanocomposites with mechanically reinforced lightweight materials show promising applications in the field of aerospace materials.

Nanocomposites are typically classified based on the type of materials used as the matrix. Other types of classifications include the shape and material of reinforcement, such as particle reinforced, lamellar reinforced and organic/inorganic reinforced. This chapter briefly summarizes the synthesis and properties of metal matrix nanocomposites (MMNCs), polymer matrix nanocomposites (PMNCs) and ceramic matrix nanocomposites (CMNCs).

17.2 Metal Matrix Nanocomposites (MMNCs)

Recently, the Inter-governmental Panel on Climate Change (IPCC) reported that aviation would account for 15 % of total greenhouse gas emissions by 2050. This emphasizes the need for developing ultra-lightweight airframe and engine materials to minimize the fuel consumption and operational cost, and to increase the payload and engine thrust. Among different materials, lightweight metal matrix composites (MMCs) are most promising because of the availability of mature processing techniques and the ability to tailor attractive properties such as specific strength, specific modulus, high thermal stability and wear resistance.

MMCs have typically micron-scale particles or whiskers, or long or short fibres in the metal matrix. When the size scale of reinforcements is selected to be in the nanometer range (typically less than 100 nm), the MMCs become MMNCs. The main advantage of using nanoscale reinforcements is that the required volume fraction of reinforcement is relatively much less (1–5 %) than that required for MMCs to obtain similar strength properties. The low volume fraction of nanoscale reinforcements in MMNCs has the benefit of retaining metallic matrix characteristics such as electrical and thermal conductivities, toughness, machinability and damping capacity.

17.2.1 Strengthening Mechanisms

Many mechanisms contribute to the strengthening of MMNCs. However, they are not additive since there is an interdependence of different mechanisms and also the dominance of one or more mechanisms over others. The brief description of each strengthening mechanism is presented below:

Grain size strengthening The grain size of the matrix in MMNCs is determined mainly by the size and volume fraction of the reinforcement. Increasing volume fractions and/or decreasing the size of the particles restrict grain growth by grain boundary pinning effects. The combined equation using the Zener and Hall–Petch

relations explains the effects of particle size (d_p) and volume fraction (v_p) on the yield strength (σ_y) of MMNCs, which is as follows: [1–3]

$$\sigma_y = \sigma_o + \frac{k_y}{\sqrt{\frac{4\alpha d_p}{3v_p}}} \quad (17.1)$$

where σ_o is the original strength of the matrix material (MPa) and k_y and α are constants. The square root term in the equation, as proposed by Zener, is related to the matrix grain size refinement.

Orowan and dislocation strengthening The strengthening effect from the Orowan mechanism (particle cutting or looping around particles by dislocations) depends on the particle geometrical characteristics and inter-particle spacing, and is generally expressed as [2, 3]

$$\sigma_{\text{orowan}} = \frac{(kMGb) \ln \frac{d_p}{b}}{\lambda \sqrt{1 - \nu}} \quad (17.2)$$

where k is a constant, M is the mean orientation factor, G is the shear modulus of the matrix, b is the Burgers vector, d_p is the particle size, ν is Poisson's ratio and λ is the interparticle spacing.

The above equation shows the significance of small particle size in improving the strength of the composites. It is also reported that the same mechanism helps in improving the creep strength of Mg (AS41/Al₂O₃) nanocomposites despite grain refinement by nanoparticles, which is undesirable with respect to creep failure [4].

On the other hand, the Orowan strengthening effect does not improve the strength linearly with decreasing particle size in the nanoscale range: there exists a critical size below which Orowan strengthening effects become insignificant because of the fact of easier particle shearing by dislocations; and this critical (nano) size is independent of the volume fraction of particles. For instance, the contribution of Orowan strengthening decreased abruptly below the critical particle size of 1.74 nm in Mg/Al₂O₃ composites [5].

Dislocation strengthening is facilitated in MMNCs by the formation of geometrically necessary dislocations (GNDs). The mismatches in the coefficient of thermal expansion and elastic modulus between the matrix and particles are mainly responsible for the formation of GNDs during processing. The dislocation forest around the particle/matrix interfaces causes severe work hardening during deformation, resulting in significant strengthening. The individual contributions of thermal mismatch (σ_{CTE}) [6, 7], elastic mismatch (EM) [8] and work hardening (σ_w) [9] on the strength of MMNCs are expressed as follows

$$\sigma_{\text{CTE}} = M\beta Gb \sqrt{\frac{A \Delta\alpha \Delta T v_p}{b d_p (1 - v_p)}} \quad (17.3)$$

$$\sigma_{EM} = C\alpha Gb \frac{1.9 v_p \varepsilon}{d_p^3} \quad (17.4)$$

$$\sigma_w = CGb \sqrt{\frac{\varepsilon}{b\dot{x}}} \quad (17.5)$$

where M is the Taylor factor, α , β , C and A are constants, G is the shear modulus of the matrix, b is the Burger's vector, $\Delta\alpha$ is the difference between the coefficient of thermal expansion between the matrix and reinforcements, ΔT is the difference between the processing and ambient temperatures, d_p is the particle size, v_p is the volume fraction, ε is the strain caused by work hardening, and \dot{x} is the average distance that dislocations move during deformation.

Load bearing effect The load bearing effect of very stiff particles contributes to the strengthening of MMNCs when the interfaces between the matrix and particles are sufficiently strong. The particle volume fraction (v_p) and the particle aspect ratio (l/t) are the critical factors deciding the load bearing efficiency of the particles. The contribution of load bearing ability of particles to the strengthening of MMNCs is expressed as [10]

$$\sigma_w = v_p \sigma_m \frac{(l+t)}{4t} \quad (17.6)$$

where l , t and σ_m are respectively the length and thickness of the particles and the matrix yield strength.

17.2.2 Synthesis and Processing

Conventional MMC processing methods are inappropriate for fabricating MMNCs because of the size scale of the reinforcements. Nanoscale sizes provide high surface areas of the reinforcements, increasing their reactivity and a tendency for agglomeration during processing. These result in an inhomogeneous reinforcement distribution in the matrix and undesirable brittle phases when conventional processing techniques are used. Therefore special processing techniques have been developed to synthesize and process MMNCs. We briefly discuss the state-of-the-art of these technologies in the following subsections.

Spark plasma sintering Conventional consolidation processes (cold compaction and sintering, pressure sintering, die casting) cannot be used to make MMNCs, owing to many problems such as coarse microstructure, poor densification, porosity defects, prolonged processing time and high sintering temperature requirements, low strength properties, and poor interface integrity between the matrix and particles.

These problems can be easily overcome by a novel sintering technique, such as pressure assisted spark plasma sintering (SPS). SPS has many unique features such as short processing time, low sintering temperature, no prior compaction step requirements, and high heating rate that help in retaining nanostructures with better particle and matrix interface characteristics, less shrinkage and near theoretical density consolidation in MMNCs [11].

The proper selections of DC pulse voltage, current, duration, ramp rate and holding time are important to generate heat (by spark plasma, Joule heating, spark impact pressure) in the shortest possible time. SPS has typically four stages, starting with the removal of gases and then application of vacuum, followed by the application of pressure coupled with the generation of heat by resistance pulse heating, and finally ending with cooling [11].

Solidification In this process, melt spinning and/or spray or gas atomization techniques are used to produce nanosize ceramic particles by rapid solidification. The nanosize particles and wetting agents are added to the molten metal by stirring or ultrasonic mixing. Then the melt is solidified under pressure or pressure-less conditions to obtain the MMNCs.

An example produced by this method is an Al/10 vol% Al₂O₃ (50 nm) nanocomposite, which showed high wear resistance and strength properties (yield strength ~515 MPa), owing to matrix grain refinement, dislocation strengthening and grain boundary pinning effects by the nanoparticles. Compared to an Al/46 vol % Al₂O₃ (29 μm) MMC or AISI 304 stainless steel, the strength is 6 or 1.5 times higher, respectively [12, 13].

Liquid metal infiltration In this process, the reinforcement particles are bonded using binders and additives to make a preform consisting of a network of interconnected pore structures. The preform is then infiltrated with molten metal under very high pressure (>1 GPa) to produce an MMNC. For example, Al/CNT nanocomposites are prepared by infiltrating liquid aluminium into a carbon nanotube (CNT) preform at 800 °C under a nitrogen atmosphere [14].

Severe plastic deformation (SPD) processing SPD processes such as equal channel angular pressing (ECAP), accumulative roll bonding (ARB) and high-pressure torsion (HPT) are very popular in the field of ultra-fine grain size materials development [15]. The same processes can also be employed to fabricate MMNCs.

In SPD processing of MMNCs the matrix grains and particles are continuously fragmented. On the one hand the fragmented particles refine the matrix grains by pinning the grain boundaries, increasing the dislocation density and forming a dislocation cell structure and subgrains; while on the other hand the grain fragmentation itself helps grain refinement by forming high angle grain boundaries [15]. For example, Al/Al₂O₃/B₄C nanocomposite processed by ARB resulted in a nanograin structure with mean matrix grain size of 230 nm [15].

Friction stir processing Friction stir processing (FSP) is an advanced thermomechanical process to develop surface nanocomposites [16]. In FSP the substrate matrix material is usually given a composite coating. The coating typically consists of nanoscale particles dispersed in the same substrate matrix.

A specially designed FSP tool pin is placed on the surface of the composite layer and moved along the designated path at a predetermined tool angle and speed. The forward rotation of the pin generates heat through friction, making the matrix melt and flow behind the pin, where it gets refined by severe plastic deformation. Subsequently, the melt is rapidly cooled under hydrostatic pressure to yield the composite with nanosize matrix grains containing nanosize particles [17]. The number of passes, the tool rotation speed, the penetration depth and the forward motion speed are the most important parameters deciding the matrix grain size and particle distribution in the nanocomposites.

Other methods Techniques such as electro-codeposition, disintegrated melt deposition, selective melting, microwave sintering, in situ composite formation by liquid metallurgical processes, melt stirring high-pressure die casting, arc discharge plasma method, high intensity ultrasound cavitation-based casting, hot extrusion, rheocasting and squeeze casting, are reported to be used either alone or in combination to prepare MMNCs [18].

17.2.3 Current Developments in Lightweight MMNCs

The combinations of lightweight matrixes such as Al, Mg and Ti with nanoscale particles of oxides (Al_2O_3 , Y_2O_3 , ZrO_2 , SiO_2), carbides (SiC , B_4C , TiC), nitrides (Si_3N_4 , AlN), borides (TiB_2) and carbon nanotubes (CNT) are promising in aerospace applications because of very high specific strength, specific stiffness and thermal stability.

Typical properties of potential Al, Mg and Ti matrix nanocomposites are presented in Table 17.1. CNT-based lightweight MMNCs are given much attention because of the extraordinarily high strength and elastic modulus of CNTs (~ 10 GPa and ~ 1 TPa respectively), very high thermal and electrical conductivity, low density (1.3 g/cm^3) and low cost.

17.3 Polymer Matrix Nanocomposites (PMNCs)

High performance polymer nanocomposites are fabricated using nanosize organic and/or inorganic additives in a polymer matrix, and show superior properties compared to traditional PMCs. The enhanced properties of polymer nanocomposites can be mainly attributed to the high surface-area/volume ratio of the

Table 17.1 Aluminium and magnesium matrix MMNCs for aerospace applications [19–28]

Composite type	Process	Particle size (nm)	Proof stress (MPa)	Ultimate tensile strength (MPa)	Elongation (%)	Hardness	Compressive strength (MPa)	Flexural strength (MPa)
Al-20 wt% TiB ₂	High energy ball milling followed by spark plasma sintering, hot extrusion	–	480	540	1.4	180 Hv	–	–
Al(5356)–B ₄ C	Cryo-milling followed by spark plasma sintering	–	–	–	–	244 Hv	–	707
Al(5083)–10 wt% SiC (Bathula)	High energy ball milling followed by spark plasma sintering	–	–	–	–	250 Hv	–	824
Al (A356)–3.5 vol % SiC	Vortex stir casting	50	145	283	3.6	75 BHN	–	–
Al-5 vol% Al ₂ O ₃	Mechanical milling followed by hot isostatic pressing and vacuum hot pressing	50	515	–	–	–	628	–
Al-5 wt% Si-4 vol % multiwall CNT	Attritor milling followed by hot rolling	70	520	–	5	–	–	–
Al-2.5 wt% CNT	Spark plasma extrusion	–	–	–	–	99 Hv	415	–
Al(2024)-2 vol% MWCNT	Mechanical alloying followed by hot pressing	–	770	–	–	245 Hv	810	–
Mg-2 wt% Al ₂ O ₃	Gravity die casting followed by hot rolling	–	200	218	–	–	–	–
AZ31 Mg alloy-2 wt% Al ₂ O ₃	Gravity die casting followed by hot rolling	–	290	306	–	–	–	–
Mg-0.66 wt% B ₄ C	Compaction followed by microwave sintering, hot extrusion	50	120	164	10	–	335	–

(continued)

Table 17.1 (continued)

Composite type	Process	Particle size (nm)	Proof stress (MPa)	Ultimate tensile strength (MPa)	Elongation (%)	Hardness	Compressive strength (MPa)	Flexural strength (MPa)
Mg-0.92 wt% Al 0.66 wt% B ₄ C	Compaction followed by microwave sintering, hot extrusion	50	130	238	7	–	356	–
Mg-1.11 vol% Al ₂ O ₃	Powder metallurgy followed by hot extrusion	50	194	250	7	–	–	–
Mg-0.66 vol% Y ₂ O ₃	Disintegrated melt deposition followed by hot extrusion	29	312	318	6.9	–	–	–
Mg-0.66 vol% ZrO ₂	Disintegrated melt deposition	29–68	221	271	4.8	–	–	–
Mg-0.54 vol% SiC	Ultrasonic cavitation casting	50	127	212	8	–	–	–
Mg-28 vol% Zn- 5 vol% Ca-1.5 vol % Al ₂ O ₃	Disintegrated melt deposition	50	750	780	2.6	–	–	–
AZ31 Mg alloy- 1.5 vol% Al ₂ O ₃	Disintegrated melt deposition followed by hot extrusion	50	219	308	14.5	–	–	–
AZ61 Mg alloy- 0.8 vol% SiO ₂	Powder metallurgy followed by hot extrusion	20	330	379	7	–	–	–
AZ91D Mg alloy- 15 vol% SiO ₂	Rheocasting followed by extrusion	150	257	289	0.7	–	–	–
ZK60A Mg alloy- 1 vol% Al ₂ O ₃	Disintegrated melt deposition followed by hot extrusion	50	158	266	19.4	–	577	–
AZ31/AZ91 alloy- 1.5 vol% Si ₃ N ₄	Disintegrated melt deposition followed by hot extrusion	50	232	331	13.1	–	517	–
Ti-0.35 mass% CNT	Spark plasma sintering followed by hot extrusion	10	592	742	26	–	–	–

reinforcement phase obtained from nanoparticles, which show a dramatic change in both physical and chemical properties [29].

The properties that show substantial improvements in a nanocomposite over the traditional filler polymers include mechanical strength, electrical conductivity, thermal stability, flame resistance, moisture resistance and chemical stability.

The aspect ratio of the nano-reinforcement and the degree of mixing between two phases are the two major factors crucial for controlling the overall properties of the composite [30]. Uniform dispersion of the nanoparticles in the polymer matrix enables homogeneity of properties and interaction of nanoparticles for superior mechanical strength. A high aspect ratio of the nanoparticles aids in improved adhesion at the nanoparticle–polymer interface [31].

17.3.1 Reinforced Strengthening

Nanomaterial reinforcements enhance the structural strength of a PMNC composite by allowing a transfer of load between them while closely bonded to the relatively soft polymer. Depending on the morphology and aspect ratio of nanomaterials, overall or directional strengthening can be achieved. Some of the nanomaterial morphologies currently being studied include nanoparticles, nanofibres, fullerenes, nanotubes and nanowires. The type of reinforcement used is broadly classified as fibrous, layered, and particles [32, 33].

Carbon and glass nanofibres are some of the most commonly used fibrous reinforcements which impart directional strength to the nanocomposites. Aramid fibres, which are commonly known as Kevlar, are also being used extensively for high-performance applications [32]. Graphite and organosilicates are some of the layered structures used as reinforcement due to their high aspect ratio. Nanoparticles of silica, carbon, metals and hard ceramics are used as particle reinforcements.

Carbon nanotube reinforcement Carbon nanotubes (CNTs) are cylindrical nanostructures of carbon with very high aspect ratios. They consist of tubes of graphene with nanometre-scale thickness and centimetre scale lengths. Typically, CNTs have one-atom-thick walls, but depending on the type of CNT used there may be multiple layers. Therefore CNTs can be classified as single-walled or multi-walled structures. CNTs are traditionally fabricated using chemical vapour deposition, arc discharge and laser ablation [34].

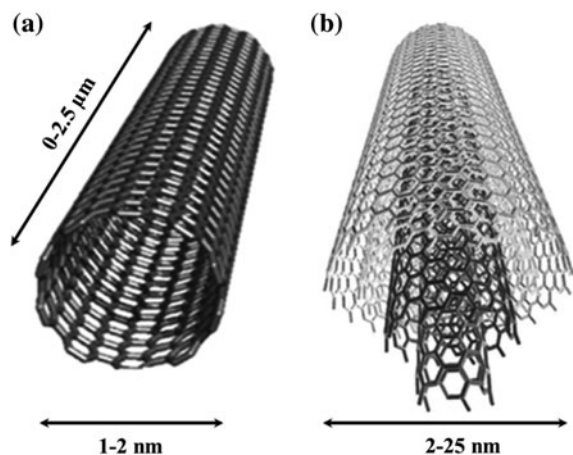
During the process of reinforcement a uniform dispersion of CNTs in the polymer matrix is essential [35–37]. Owing to van der Waals interactions, CNTs tend to aggregate during the mixing process, which could lead to an inhomogeneous strength distribution. Inefficient transfer of load through the material could lead to crack sites in the nanocomposite. Uniform dispersion of CNTs is also essential for electrical and thermal conductivity of the nanocomposites. CNTs are inherently hydrophobic in nature, but recent progress on chemical attachment to reduce the hydrophobicity has helped improve the adhesion to polymers [38–40].

Single-walled and multi-walled CNT reinforcements show different properties in a composite. Single-walled CNTs are graphene wrapped in a hollow cylindrical geometry, whereas multi-walled CNTs can be multiple concentric tubes or a scroll of graphene. CNTs tend to grow in a multi-walled geometry and therefore it is challenging to grow only single-walled nanotubes (Fig. 17.1). Due to the relatively smaller size, single-walled CNTs have a higher tendency to aggregate during the mixing process. Although multi-walled CNTs show a relatively lower agglomeration during the mixing process, they tend to show lower mechanical strength compared to single-walled CNTs. Double-walled CNTs have properties similar to those of a single-walled CNT but also have improved surface chemical resistance, which helps in chemical modification to improve the adhesion with the polymer.

Cadek et al. have shown an increase in Young's modulus by a factor of 1.8 and hardness by a factor of 1.6 in a multi-walled CNT/polyvinyl alcohol nanocomposite with 1 wt% of CNTs. It was also observed that the presence of nanotubes acts as a nucleation site for the crystallization of polyvinyl alcohol. Increased crystallinity of the polymer matrix has been shown to improve the mechanical strength of the nanocomposite [41]. Gojny et al. studied the enhancement of stiffness and fracture toughness of low carbon content CNT-reinforced epoxy. It was observed that compared to carbon black-reinforced epoxy, a relatively small amount (0.1 wt%) of CNTs resulted in a higher tensile strength and Young's modulus [42]. Kearns et al. showed that single-walled CNTs at 1 wt% content had 40 % higher tensile strength and 55 % higher Young's modulus compared to neat polypropylene fibres [43].

Carbon nanofibre reinforcement Carbon nanofibres (CNF) are cylindrical nanostructures of stacked cones of graphite. CNFs have a diameter typically ranging from 10 to 50 nm and can be few hundred microns long. CNFs have higher surface-area/volume ratios compared to a traditional carbon fibre. Higher surface area aids in better adhesion to the polymer and efficient load transfer characteristics. The ultimate tensile strength of a nanocomposite with CNFs is higher than that

Fig. 17.1 Schematic of **a** single-walled CNT with nanometer-scale width and high aspect ratio and **b** multi-walled CNT with relatively higher width showing concentric tubes



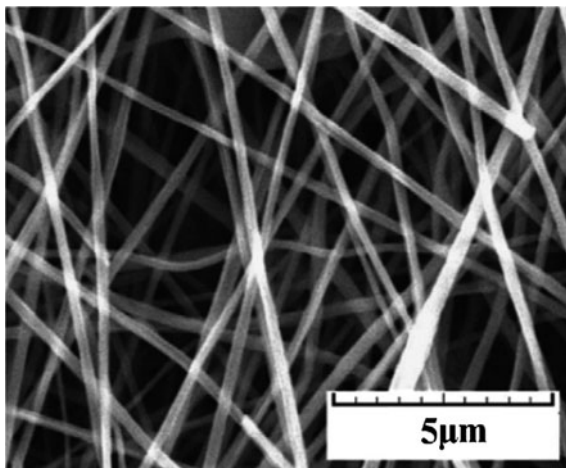
obtained from PMCs using traditional carbon fibres. This has been attributed to lower defects in the nanofibres and higher contact area with the polymer. CNFs also show higher flexibility due to the higher aspect ratio, which leads to superior mechanical properties.

Carbon nanofibres are typically fabricated from poly-acrylonitrile or pitch polymers. The polymer precursors are initially spun or drawn into filaments. This process aligns the polymer chains in one direction to have enhanced mechanical properties along the longitudinal direction. The filaments are then heated to a temperature of 1700 °C in a process known as carbonization or graphitization. This process evaporates or sublimates all the non-carbon atoms from the polymer, thereby producing the carbon fibre. Figure 17.2 shows a scanning electron micrograph of CNFs produced using a poly-acrylonitrile precursor.

CNFs can also be fabricated using pyrolysis of methane at 900 °C in the presence of a metal catalyst. Pyrolysis of hydrocarbons is one of the most studied methods to grow carbon fibres and could possibly be used for mass production at relatively low cost. Some of the other techniques for producing CNFs are template synthesis, electrospinning, phase separation, etc. [44, 45].

CNFs have superior mechanical and electrical properties compared to traditional carbon fibres. Vapour-grown CNFs by Endo et al. have shown that the tensile strength of a nanocomposite is inversely proportional to the diameter of the nanofibres. A tensile strength of 2 GPa and a tensile modulus of 200 GPa was observed [46]. Also, in contrast to CNT-reinforced nanocomposites, nanofibres have lower probability of aggregation and thus produce a homogeneous composite.

Fig. 17.2 SEM micrograph of poly-acrylonitrile-based carbon nanofibres



CNF-reinforced nanocomposites typically are also reinforced with CNTs for tandem properties and smoother surface finish.

Other reinforcements There are other materials such as exfoliated graphite, nano-structured titanium oxide, aluminium oxide, silica, polyhedral oligomeric silsesquioxane (POSS), montmorillonite nanoclays and silicon carbide (SiC) that have been used to form polymer nanocomposites with enhanced material properties.

17.3.2 Fabrication of PMNCs

Fabrication of PMNCs can be done using conventional composite methods. Some of the most widely used fabrication processes include wet lay-up, resin transfer moulding (RTM), vacuum assisted RTM, filament winding, resin film infusion, prepreg moulding, and autoclave processing [47].

Wet lay-up and pultrusion process This involves positioning layers of reinforcement material in or against a mould. These layers are then impregnated with a liquid resin system, either with a brush or roller, to ensure a good wet-out of the reinforcement material. Layering and impregnation are repeated until the required thickness is achieved.

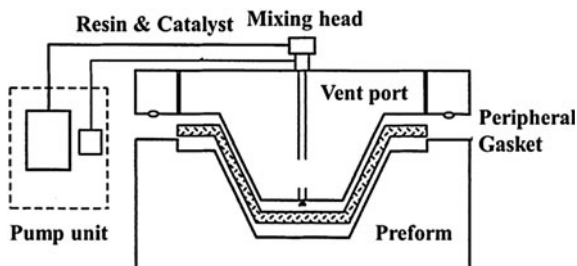
Curing can be performed at room temperature or under heat, depending on the resin system. This can be accomplished with or without the use of a vacuum bagging process. The mechanical properties of products are, however, usually poor due to the presence of voids and non-uniformity.

Pultrusion is similar to the wet lay-up process in terms of applying liquid resin and impregnation, but it is a process of producing a continuous length of reinforced polymer nanocomposites with constant cross-section. Mass production at relatively low cost can be achieved using this method. The amounts of voids and defects in this process are similar to those from the wet lay-up process. The fibre alignment in the composite can be optimized by varying the rate at which the fibres are pulled, the temperature, and the curing time.

Resin transfer moulding and vacuum assisted RTM Resin transfer moulding is a closed-mould process that yields high reinforcement-to-resin ratio, increased laminate compression and excellent strength-to-weight characteristics [48]. In this process a nanofibre preform or dry fibre reinforcement is packed into a mould cavity with the desired shape and the mould is then closed. Low viscosity resin with catalysts for hardening is then pumped into the mould under pressure, displacing the air at the edges until the mould is filled. The nanocomposites are then cured by heating to polymerize the resin into a rigid plastic. The shape and preparation methods of nanofibre preforms can also have a significant influence on the final properties of the nanocomposite. CNFs weaved into a fabric shows higher toughness than unidirectional fibres.

Vacuum-assisted RTM is also a closed-mould process using a partial vacuum to assist the resin flow. Vacuum assists in allowing air bubbles to escape and in

Fig. 17.3 Schematic of the vacuum-assisted resin transfer moulding process



eliminating voids in the final composite. It also helps a homogeneous resin flow through the nanofibre preform. Figure 17.3 shows a schematic of the vacuum-assisted RTM process.

Resin film infusion consists of a catalyzed semi-solid resin layered with the nanofibre preform in a vacuum mould. Vacuum eliminates any air in the mould to avoid air bubbles in the composite, and then the mould is heated in an autoclave. The resin is melted and impregnated into the preform and then polymerized to form a rigid plastic.

Filament winding and prepreg moulding Filament winding is typically used to fabricate hollow structures. A steel mandrel is rotated along its axis and carbon fibre impregnated with resin is wound on the mandrel. Carbon fibre is wound at different angles and orientations on the mandrel to achieve complex patterns for higher strength and toughness. The mandrel plus the desired thickness of nanocomposite is then cured, and the hollow structure is separated from the mandrel. Various process parameters like tension on the fibres, rate of mandrel rotation, resin concentration, nanoparticle reinforcement in the resin, and curing temperature can be used to optimize the final properties. Mass production of hollow nanocomposite structures is feasible using this process.

Prepreg composites consist of nanofibre reinforcements that have been pre-impregnated with a resin. The resins are usually pre-catalyzed and semi-cured for ease of handling at ambient temperatures. High-temperature annealing is usually required to achieve complete polymerization. The prepregs are placed in vacuum moulds having the desired configuration and are heated to allow the resin to soften. This helps the resin to reflow into the prepreg structure, and then the temperature is increased to completely cure the structure.

17.3.3 Current Challenges in PMNCs

PMNCs show promising improvements in material properties in contrast to the conventional counterparts. Relatively lower cost, and significant improvements in strength, toughness and electrical conductivity, are only a few among many properties that can be obtained using polymer nanocomposites.

Homogeneous dispersion and wettability of the nanoparticles and large-scale production of nanostructures is still being intensively researched [49]. The control of porosity during polymer pouring and densification affects the final properties. Formation of agglomerates could cause splitting of the nanocomposite when subjected to force. The (mis)orientation of carbon nanofibres in a unidirectional composite could also lead to crack initiation.

17.4 Ceramic Matrix Nanocomposites (CMNCs)

Ceramic matrix nanocomposites (CMNCs) are nanostructured metal, metal oxides and ceramics reinforced in a ceramic matrix. CMNCs exhibit improved fracture toughness, thermal stability, resistance to corrosion and show lower brittleness in contrast to conventional ceramics.

CMNCs can be classified into two groups based on grain size of the matrix phase: (i) the micro-nano type, where the matrix is composed of micrometre-sized grains with a nanometre reinforcement [50] and (ii) the nano-nano type, also referred to as nanoceramics. This second group contains nano-sized (<100 nm) constituents of both the matrix and reinforcement. A dramatic difference in properties is observed for these two groups of composites.

17.4.1 Types of Reinforcement/Strengthening Mechanisms

Conventional ceramic matrix composites use SiC, Si₃N₄, TiC, etc., as reinforcement. Although the reinforcements are hard and brittle, sufficient improvement in the strength and fracture toughness of the composite is observed. Soft reinforcements like graphite and metal nanoparticles also have shown improved overall properties [51–53]. Current research interest focusses on both hard and soft reinforcements on the nanometre scale and nanostructures with high aspect ratios.

Metal nanoparticle-reinforced CMNCs Enhanced mechanical and structural properties are obtained by reinforcing the ceramic matrix with nano-sized metal particles. Typically ceramics such as silica, silicon carbide, alumina, zirconia, mullite, etc., are used as ceramic matrix phase materials. Nanoparticles of tungsten, molybdenum, nickel, chromium, iron, etc., are used as reinforcement.

Powder processing techniques such as hot pressing or cold pressing and high-temperature sintering are used to fabricate CMNCs. Precursors for both matrix and reinforcement phases start as nanopowders; the desired proportions of metal and ceramic powders are mixed and hot pressed, allowing consolidation and sintering [54–60]. Besides simple powder mixing, the nanocomposites can also be made using oxide reduction, sol–gel, gel casting and salt infiltration.

Niihara et al. fabricated $\text{Al}_2\text{O}_3/\text{Mo}$ nanocomposites using α and γ alumina. It was observed that in a 5 vol% Mo system, elongated grains of Mo surrounded alumina grains, resulting in improved fracture toughness, hardness and strength of the nanocomposite. Ceramic nanocomposites containing lower melting point metals also show exceptional mechanical properties [54, 60]. Along with the mechanical properties, the magnetic properties are also expected to improve by simply incorporating nano-sized Ni, Co and Fe into an Al_2O_3 matrix.

Soft nanoparticle-reinforced CMNCs Besides the mechanical properties, the most important improvement using soft nanoparticles in CMNCs is the machinability [61–64]. One of the most studied soft reinforcements is hexagonal boron nitride (h-BN), which has excellent corrosion resistance, thermal shock resistance and machinability. Kusunose et al. [61] obtained a $\text{Si}_3\text{N}_4/\text{h-BN}$ nanocomposite with significant improvements in machinability, strength and dispersion. Also, hexagonal boron nitride nanocomposites with silicon nitride, silicon carbide and zirconia all showed property improvements over their monolithic ceramic counterparts.

It was observed that hexagonal boron nitride in the matrix inhibits grain growth during the sintering process. This yields in a finer microstructure of the nanocomposite. Although in most of these nanocomposites a decrease in toughness was observed, it was still higher than that of conventional ceramic composites. Hexagonal boron nitride also showed improvements of the thermal resistance in the silicon nitride system up to temperatures as high as 1500 °C.

Hard nanoparticle-reinforced CMNCs Hard materials such as SiC, Si_3N_4 , ZrO_2 and TiO_2 are used as reinforcements in oxide ceramic matrices like Al_2O_3 and MgO. These nanocomposites have higher sintering temperatures than the monolithic matrix materials. For example, in the $\text{Al}_2\text{O}_3/\text{SiC}$ system a dramatic increase in sintering temperatures was observed with the incorporation of 5 vol% SiC [50]. Similar to hexagonal boron nitride reinforcement, SiC promoted a fine grained microstructure. Nanoparticles of SiC with small grain size appeared to disperse in the matrix: however, large grains were dispersed along the grain boundary. SiC incorporation led to higher toughness and strength and this could be mainly because of the residual stress generated due to the difference in thermal expansion coefficients of Al_2O_3 and SiC [50].

Carbon nanotube (CNT)-reinforced CMNCs Carbon nanotube reinforced CMNCs are known to impart very high toughness to nanocomposites. CNTs are lightweight, hollow and high aspect ratio materials, see Sect. 17.3.1 for an introduction on CNTs. CNT reinforcement gives improved high temperature strength, toughness and electrical properties.

Ceramic matrices are brittle and stiff and the main purpose of reinforcement is to impart toughness. CNTs enhance the fracture toughness and also enable electrical conductivity in ceramics. However, significant improvements in the properties of ceramic nanocomposites have not been observed using CNTs. Only a limited amount of the CNTs' potential has been exploited, and more research is needed.

The critical parameters that affect the properties of CNT-reinforced CMNCs are the type of CNT, the sintering process, and the homogeneous dispersion and bonding of CNTs to the matrix material for an efficient load transfer.

17.4.2 Fabrication of CMNCs

CMNCs are fabricated using a wide range of techniques such as sol–gel, hot pressing, hot isostatic pressing, cold pressing and sintering, oxide reduction, salt infiltration, SPS, micro emulsion, auto ignition, codeposition, microwave sintering, etc. Dense CMNCs can be obtained using hot pressing: however, consolidation to high densities and the high sintering temperatures are still major difficulties.

Sol–gel and gel casting The sol–gel technique uses an innovative approach towards processing of ceramic structures. Suitable precursors are polymerized to form a colloidal solution known as a sol. Typically the precursors for preparation of sols include metal oxides or alkoxides which are subject to hydrolysis polymerization to form the sols. The liquid state then goes through hydrolysis or condensation at relatively high temperatures to form gels. Sintering of these gels at relatively high temperatures (lower than powder processing) yields dense ceramic composites. This sintering process and temperatures of the gels can be used to alter the structure and properties of the nanocomposites. Thin films of ceramics can also be produced by spray pyrolysis of gels. Relatively low processing temperatures and better control over homogeneity and particle distribution are some of the advantages of using this process. However, coarsening of the microstructure occurs during the sintering process, and this could lower the overall strength.

Hot pressing Powder mixing and consolidation is one of the simplest ways to fabricate CMNCs. This involves conventional mixing and/or milling processes, followed by compaction or consolidation and then densification (sintering and/or pressing). These powder processing techniques include hot pressing and hot isostatic pressing, where the compaction and sintering occur simultaneously. Similar to the sol–gel process, coarsening of grains during sintering could lower the overall strength of the nanocomposite. Depending on the size and shape of powder and the process used for compaction, complete densification is difficult to achieve. Metal powders during sintering at high temperatures have the tendency to oxidize and may also cause differences in the strength of the nanocomposite.

Other methods Some of the techniques such as oxide reduction, salt infiltration and SPS are also used in fabricating CMNCs. Similar to conventional powder processing, the oxide reduction process utilizes metal oxide powders in a ceramic matrix phase. During sintering the metal oxide particles are reduced to the metallic state in the presence of a reducing agent.

Salt infiltration utilizes the reduction of metal salts to metal nanostructures in the porous ceramic matrix. The ceramic matrix phase is produced using conventional powder compaction and sintering processes. The powder processing conditions are optimized to

achieve a network of pores without complete densification. The pores are infiltrated using a water-based metal salt solution and then dried to eliminate any water, leaving the dispersed metal salts in the pores of the nanocomposite. Annealing in a reducing atmosphere causes the metal salts to change the oxidation state to the metallic form.

17.5 Characterization of Nanocomposites

High resolution characterization tools such as the scanning electron microscope (SEM), transmission electron microscope (TEM), scanning tunnelling microscope (STM), atomic force microscope (AFM), X-ray diffraction (XRD), energy dispersive X-ray spectroscopy (EDAX), and focussed ion beam (FIB) techniques are generally used to assess the phases, morphologies and microstructures of nano-scale particle reinforced composites [17].

AFMs are widely used in developing MMNCs. An AFM is usually operated in three modes: (1) contact mode, (2) non-contact mode and (3) phase mode to analyze MMNCs. Both the contact and non-contact modes are used to obtain high resolution topographic images of the surfaces of MMNCs, whereas the phase mode provides the surface mapping of material composition [17].

An STM is generally used to obtain the atomic arrangements of the surfaces of MMNCs [17]. Electron microscopes (SEM with EDS, TEM) are also used to obtain surface topographies, phase identifications, composition maps, crystallographic orientations, electronic structure and phase shift. The grain sizes are commonly determined from XRD patterns.

Most of the characterization tools mentioned for MMNCs are the same for PMNCs and CMNCs. However, some of the techniques such as STM and conductive AFM require the material to be electrically conductive and thus could cause limitations due the lack of conductivity in CMNCs and PMNCs.

Various other techniques for characterization of PMNCs include wide-angle X-ray diffraction (WAXD), small-angle X-ray scattering (SAXS), scanning probe microscopy (SPM), differential scanning calorimetry (DSC), thermo gravimetric analysis (TGA), Fourier transform infrared spectroscopy (FTIR), and dynamic modulus analysis (DMA). Using these techniques enables obtaining a comprehensive understanding of the basic, physical, chemical and structural properties of PMNCs [65–70].

Some of the most commonly used characterization measurements for CMNCs include Vickers hardness (micro and nano hardness), impact fracture toughness, residual and fracture strength, and compressive and tensile strength.

17.6 Future Aerospace Applications

The use of MMNCs in aircraft or aero engine applications is still in the future. However, their potential has been noted by many recent researches.

MMNCs using Al, Mg or Ti matrices may find use in the next generation of aircraft, based on property improvements and weight savings. For instance, the substitution of Ti MMNCs for currently used Ni-base superalloys in the high pressure compressors of jet engines is one potential application where weight savings of more than 50 % are expected [71]. Other possible applications include helicopter rotor blades, vertical fins, fan guide exit vanes, turbine fan blades and discs, engine spacers and shafts, brake pads and brake discs, compressor rotor blisks and blings.

In recent years, PMNCs for aerospace applications have shown significant improvements in mechanical properties. PMNCs are being used by Boeing as high temperature materials in aerospace applications [72]. Researchers have developed lightweight and durable transparent nanocomposites for the aerospace industry [73].

CMNCs are being used in space applications owing to lower weight and high thermal stability. They are also being used in gas turbine components, brake pads and thrust control pads in jet engines. SiC/C CMNCs were proposed for steering flaps for the NASA space vehicle X-38 [74] which, however, was cancelled in 2002.

17.7 Conclusions

Although nanocomposites have the potential to provide exceptionally high strength, stiffness, wear resistance, thermal conductivity and significant weight savings, the major challenges such as aerospace product quality standard, reproducibility, machining, immature processing techniques, high capital investment for fabrication, and poor ductility and fracture characteristics should be addressed to obtain a wide commercial acceptance in aerospace applications. Research in the field on nanocomposites is very broad and in the early stages of development: more research and in-depth understanding of every process is required to optimize the conditions for fabrication of nanocomposites.

Acknowledgments One of this chapter's authors, Naveen Mahenderkar, would like to thank Dr. N. Eswara Prasad, Director, DMSRDE, Kanpur, India for giving the opportunity to contribute to this book series, and also for his valuable guidance and encouragement. T. Ram Prabhu would like to thank Dr. K. Tamilmani, DG (Aero), DRDO and Shri P. Jayapal, Chief Executive (A), CEMILAC, DRDO for their constant encouragement and support.

References

1. Witkin D, Lee Z, Rodríguez R, Nutt S, Lavernia E (2003) Al–Mg alloy engineered with bimodal grain size for high strength and increased ductility. *Scr Mater* 49:297–302
2. Ye J, Han BQ, Lee Z, Ahn B, Nutt SR, Schoenung JM (2005) A tri-modal aluminum based composite with super-high strength. *Scr Mater* 53:481–486
3. Sanaty-Zadeh A (2012) Comparison between current models for the strength of particulate-reinforced metal matrix nanocomposites with emphasis on consideration of Hall-Petch effect. *Mat Sci Eng A* 531:112–118

4. Kumar H, Chaudhari GP (2014) Creep behaviour of AS41 alloy matrix nano-composites. *Mater Sci Eng A* 607:435–444
5. Zhang Z, Chen DL (2008) Contribution of orowan strengthening effect in particulate-reinforced metal matrix nanocomposites. *Mater Sci Eng A* 483–484:148–152
6. Hassan SF, Tan MJ, Gupta M (2008) High-temperature tensile properties of Mg/Al₂O₃ nanocomposite. *Mater Sci Eng A* 486:56–62
7. Kapoor R, Kumar N, Mishra RS, Huskamp CS, Sankaran KK (2010) Influence of fraction of high angle boundaries on the mechanical behaviour of an ultrafine grained Al–Mg alloy. *Mater Sci Eng A* 527:5246–5254
8. Tun KS, Gupta M (2007) Improving mechanical properties of magnesium using nano-yttria reinforcement and microwave assisted powder metallurgy method. *Compos Sci Technol* 67:2657–2664
9. Li Y, Zhao YH, Ortalan V, Liu W, Zhang ZH, Vogt RG, Browning ND, Lavernia EJ, Schoenung JM (2009) Investigation of aluminum-based nanocomposites with ultra-high strength. *Mater Sci Eng A* 527:305–316
10. Nguyen QB, Gupta M (2010) Enhancing compressive response of AZ31B using nano-Al₂O₃ and copper additions. *J Alloys Compd* 490:382–387
11. Saheb N, Iqbal Z, Khalil A, Hakeem AS, Aqeeli N, Laoui T, Al-Qutub A, Kirchner R (2012) Spark plasma sintering of metals and metal matrix nanocomposites: a review. *J Nano Mater* 2012:1–13
12. Jun Q, Linan A, Blau PJ (2006) Sliding friction and wear characteristics of Al₂O₃–Alnanocomposites. Paper No. IJTC2006-12326 in: Proceedings of STLE/ASME Intenational Joint Tribology Conference, IJTC 2006, 23–25 October 2006, San Antonio, TX, USA, pp 59–60
13. Rohatgi PK, Schultz B (2007) Lightweight metal matrix nanocomposites—stretching the boundaries of metals. *Mater Matters* 2:16
14. Zhou S, Zhang X, Ding Z, Min C, Xu G, Zhu W (2007) Fabrication and tribological properties of carbon nanotubes reinforced Al composites prepared by pressureless infiltration technique. *Compos A* 38:301–306
15. Beni HA, Alizadeh M, Ghaffari M, Amini R (2014) Investigation of grain refinement in Al/Al₂O₃/B₄C nano-composite produced by ARB. *Compos B* 58:438–442
16. Mazahery A, Shabani OS (2013) Plasticity and microstructure of A356 matrix nano composites. *J. King Saud Univ. – Eng. Sci.* 25:41–48
17. Gan YX (2012) Structural assessment of nanocomposites. *Micron* 43:782–817
18. Casati R, Vedani M (2014) Metal matrix composites reinforced by nano-particles—a review. *Metals* 4:65–83
19. Sadeghian Z, Lotfi B, Enayati MH, Beiss P (2011) Microstructural and mechanical evaluation of Al-TiB₂ nanostructure composite fabricated by mechanical alloying. *J Alloys Compd* 509:7758–7763
20. Vintila R, Charest A, Drew RAL, Brochu M (2011) Synthesis and consolidation via spark plasma sintering of nanostructured al-5356/B₄C composite. *Mater Sci Eng A* 528:4395–4407
21. Mazaheri Y, Karimzadeh F, Enayati MH (2011) A novel technique for development of A356/Al₂O₃ surface nanocomposite by friction stir processing. *J Mater Process Technol* 211:1614–1619
22. Prabhu B (2005) Microstructural and mechanical characterization of Al–Al₂O₃ nanocomposites synthesized by high-energy milling. M.S. Thesis, University of Central Florida, Orlando, FL, USA
23. Choi HJ, Shin JH, Min BH, Bae DH (2010) Deformation behaviour of Al–Si alloy based nanocomposites reinforced with carbon nanotubes. *Compos A* 41:327–329
24. Morsi K, Esawi AMK, Lanka S, Sayed A, Taher M (2010) Sparkplasma extrusion (SPE) of ball-milled aluminium and carbon nanotube reinforced aluminium composite powders. *Compos A* 41:322–326
25. Jafari M, Abbasi MH, Enayati MH, Karimzadeh F (2012) Mechanical properties of nanostructured Al₂O₃–MWCNT composite prepared by optimized mechanical milling and hot pressing methods. *Adv Powder Technol.* 23:205–210

26. Korayem MH, Mahmudi R, Poole WJ (2013) Work hardening behaviour of Mg-based nano-composites strengthened by Al₂O₃ nano-particles. *Mater Sci Eng A* 567:89–94
27. Kondoh K, Threrujirapong T, Imai H, Umeda J, Fugetsu B (2008) CNTs/TiC reinforced titanium matrix nanocomposites via powder metallurgy and its microstructural and mechanical properties. *J Nanomater* (doi:10.1155/2008/127538)
28. Goh CS, Wei J, Lee LC, Gupta M (2007) Properties and deformation behaviour of Mg–Y₂O₃ nanocomposites. *Acta Mater* 55:5115–5121
29. Luo JJ, Daniel IM (2003) Characterization and modeling of mechanical behaviour of polymer/clay nanocomposites. *Compos Sci Technol* 63:1607–1616
30. Park C, Park O, Lim J, Kim H (2001) The fabrication of syndiotactic polystyrene/organophilic clay nanocomposites and their properties. *Polymer* 42:7465–7475
31. Gorga RE, Cohen RE (2004) Toughness enhancements in poly (methyl methacrylate) by addition of oriented multiwall carbon nanotube. *J Polym Sci Part B Polym Phys* 42:2690–2702
32. Schmidt D, Shah D, Giannelis EP (2002) New advances in polymer/layered silicate nanocomposites. *Curr Opin Solid State Mater Sci* 6:205–212
33. Thostenson E, Li C, Chou T (2005) Review—nanocomposites in context. *J Compos Sci Tech* 65:491–516
34. Liu, J., Fan, S. and Dai, H., 2004, “Recent advances in methods of forming carbon nanotubes”, *MRS Bulletin*, Pp. 244–250
35. Shaffer MSP, Windle AH (1999) Analogies between polymer solutions and carbon nanotube dispersions. *Macromolecules* 32:6864–6866
36. Gong X, Liu J, Baskaran S (2000) Surfactant assisted processing of carbon nanotube/polymer composites. *Chem Mater* 12:1049–1052
37. Jin L, Bower C (1998) Alignment of carbon nanotubes in a polymer matrix by mechanical stretching. *Appl Phys Lett* 73:1197–1199
38. Karousis N, Tagmatarchis N, Tasis D (2010) Current progress on the chemical modification of carbon nanotubes. *Chem Rev* 110:5366–5397
39. Ajayan PM, Stephan O, Colliex C, Trauth D (1994) Aligned carbon nanotube arrays formed by cutting a polymer resin nanotube composite. *Science* 265:1212–1214
40. Thostenson ET, Ren Z, Chou TW (2001) Advances in the science and technology of carbon nanotubes and their composites: a review. *Compos Sci Tech* 61:1899–1912
41. Cadek M, Coleman JN, Barron V, Hedicke K, Blau WJ (2002) Morphological and mechanical properties of carbon-nanotube-reinforced semicrystalline and amorphous polymer composites. *Appl Phys Lett* 81:5123–5125
42. Gobjny FH, Wichmann MHG, Kopke U, Fiedler B, Schulte K (2004) Carbon nanotube-reinforced epoxy-composites: enhanced stiffness and fracture toughness at low nanotube content. *Compos Sci Technol* 64:2363–2371
43. Kearns JC, Shambaugh RL (2002) Polypropylene fibers reinforced with carbon nanotubes. *J Appl Polym Sci* 86:2079–2084
44. Larrondo L, Manley R, St J (1981) Electrostatic fiber spinning from polymer melts. I. Experimental observations on fiber formation and properties. *J Polym Sci Polym Phys* 19:909–920
45. Tibbetts GG, Finegan JC, McHugh JJ, Ting J-M, Glasgow DG, Lake ML (2000) Applications research on vapor-grown carbon fibers. In: Tomanek E, Enbody RJ (eds) *Science and application of nanotubes*, Kluwer Academic/Plenum Publishers, New York, USA, pp 35–51
46. Endo M, Kim YA, Hayashi T, Nishimura K, Matusita T, Miyashita K et al (2000) Vapor-grown carbon fibers (VGCFs)—basic properties and their battery applications. *Carbon* 39:1287–1297
47. Mazumder SK (ed) (2002) *Composites manufacturing: materials, product, and process engineering*. CRC Press LLC, Boca Raton, FL, USA
48. Ormighi HJ Jr, Bolner AS, Fiorio R, Zattera AJ, Amico SC (2010) Mechanical and dynamic mechanical analysis of hybrid composites molded by resin transfer molding. *J Appl Polym Sci* 118:887–896

49. Jancar J, Douglas JF, Starr FW, Kumar SK, Cassagnau P, Lesser AJ, Sternstein SS, Buehler MJ (2010) Current issues in research on structure-property relationships in polymer nanocomposites. *Polymer* 51:3321–3343
50. Niihara K (1991) New design concept of structural ceramics: ceramic nanocomposites. *J Ceram Soc Jpn* 99:974
51. Gao L, Jin XH, Zheng S (2004) *Ceramic nanocomposites*. Chemical Engineering Publishers, Beijing, China
52. Suganuma K, Sasaki G, Fujita T et al (1993) Mechanical properties and microstructures of Machinable silicon carbide. *J Mater Sci* 28:1175
53. Mizutani T, Kusunose T, Sando M et al (1997) Fabrication and properties of nano-sized BN-particulate dispersed sialon ceramics. *Ceram Eng Sci Proc* 18:669
54. Oh ST, Lee JS, Sekino T et al (2001) Fabrication of Cu dispersed Al₂O₃ nanocomposites using Al₂O₃/CuO and Al₂O₃/Cu-nitrate mixtures. *Scr Mater* 44:2117
55. Nawa M, Sekino T, Niihara K (1994) Fabrication and mechanical behaviour of Al₂O₃/Mo nanocomposites. *J Mater Sci* 29:3185
56. Nawa M, Yamazaki K, Sekino T et al (1994) A new type of nanocomposite in tetragonal zirconia polycrystal-molybdenum system. *Mater Lett* 20:299
57. Sekino T, Niihara K (1995) Microstructural characteristics and mechanical properties for Al₂O₃/metal nanocomposite. *Nanostruc Mater* 6:663
58. Sekino T, Niihara K (1997) Fabrication and mechanical properties of fine-tungsten-dispersed alumina-based composites. *J Mater Sci* 32:3943
59. Ji Y, Yeomans JA (2002) Processing and mechanical properties of Al₂O₃-5 vol% Cr nanocomposites. *J Eur Ceram Soc* 22:1927
60. Sekino T, Nakajima T, Satoru U et al (1997) Reduction and sintering of nickel-dispersed-alumina composite and its properties. *J Am Ceram Soc* 80:1139
61. Kusunose T, Sekino T, Chao YH et al (2002) Fabrication and microstructure of silicon nitride/boron nitride nanocomposite and its properties. *J Am Ceram Soc* 85:2678
62. Li YL, Qiao GJ, Jin ZH (2002) Machinable, Al₂O₃/BN composite ceramics with strong mechanical properties. *Mater Res Bull* 38:1401
63. Li YL, Zhang JX, Qiao GJ et al (2005) Fabrication and properties of machinable 3Y–ZrO₂/BN nanocomposites. *Mater Sci Eng A* 397:35
64. Wang XD, Qiao GJ, Jin ZH (2004) Fabrication of machinable silicon carbide-boron nitride ceramic nanocomposites. *J Am Ceram Soc* 87:565
65. Meyyappan M (ed) (2004) *Carbon nanotubes: science and application*. CRC Press LLC, Boca Raton, FL, USA
66. Giannelis EP (1996) Polymer layered silicates nanocomposites. *Adv Mater* 8:29–35
67. Reichert P, Kressler J, Thomann R, Mulhaupt R, Stoppelmann G (1998) Nanocomposites based on a synthetic layer silicate and polyamide-12. *Acta Polym* 49:116–123
68. Yano K, Usuki A (1993) Synthesis and properties of polyimide-clay hybrid. *J Polym Sci Part A Polym Chem* 31:2493–2498
69. Yano K, Usuki A, Okada A, Kurauchi T (1991) Synthesis and properties of polyimide-clay hybrid. *Polymer Prep* 32:65
70. Park JH, Jana S (2003) Mechanism of exfoliation of nanoclay particles in epoxy-clay nanocomposites. *Macromolecules* 36:2758–2768
71. Singerman SA, Jackson JJ (1996) Super alloys. In: Kissinger RD, Deye DJ, Anton DL, Cetel AD, Nathal MV, Pollock TM, Woodford DA (eds) *The Minerals, Metals and Materials Society*, Warrendale, PA, USA, pp 579–586
72. Koo J, Pilato L (2005) Polymer nanostructured materials for high temperature applications. *SAMPE Journal* 41(2):7–19
73. Transparent nanocomposites for aerospace applications. *Adv Compos Bullet*, Feb 2004
74. Pfeiffer K-H, Peetz K (2002) All-ceramic body flap qualified for space flight on the X-38. In: 53rd International Astronautical Congress. 10–19 October, 2002, Houston, TX, USA